ELSEVIER

Applied Catalysis A: General 180 (1999) 399–409

APPLIED CATALYSIS A: GENERAL

A new method for enhancing the performance of red mud as a hydrogenation catalyst

Jorge Álvarez, Salvador Ordóñez, Roberto Rosal, Herminio Sastre, Fernando V. Díez*

Department of Chemical and Environmental Engineering, University of Oviedo, 33071-Oviedo, Spain

Received 22 April 1998; received in revised form 30 October 1998; accepted 5 November 1998

Abstract

A new method is presented for improving the performance of red mud as a hydrogenation catalyst (a residue from the production of alumina by the Bayer process that contains iron oxides), based on the method developed by K.C. Pratt and V. Christoverson, Fuel 61 (1982) 460. The activation method consists essentially in dissolving red mud in a mixture of aqueous hydrochloric and phosphoric acids, boiling the resulting solution, adding aqueous ammonia until pH=8, and filtering, washing, drying and calcining the resulting precipitate. The catalyst thus obtained is characterised, and after sulphidation, tested (activity and life) for the hydrogenation of a light fraction of an anthracene oil. The catalytic performance is compared with that of sulphided untreated red mud and sulphided red mud activated by the method of Pratt and Christoverson. This activation method has proved to be more effective in improving the performance of red mud as a hydrogenation catalyst than the method of Pratt and Christoverson, since the activated catalyst presents a slightly higher level of activity and a markedly extended active life.

Keywords: Red mud; Anthracene oil; Catalyst deactivation; Catalytic hydrogenation; Scanning electron microscopy; X-ray diffraction; Phosphorus promotional effect

1. Introduction

Red mud (RM) is a by-product in the manufacture of alumina by Bayer process that contains mainly oxides of iron, aluminium, titanium, silicon, calcium and sodium. Sulphided red mud is active as a hydrogenation catalyst, due to its iron sulphide content, and has been used for the hydrogenation of organic compounds [1,2], and the liquefaction of coal [2–4] and biomass [5].

Catalytic hydrogenation of anthracene oil yields a solvent with high hydrogen-donor capacity, due to its content in hydroaromatic compounds such as dihydroanthracene, dihydrophenanthrene and tetrahydrofluoranthene. Hydrogenated anthracene oil can be used in processes in which transferable hydrogen plays an important role, such as coal liquefaction [8,11], oil-coal coprocessing [10,14], and coke production by carbonisation of low-rank coals with pitch-like materials [9].

In previous works, sulphided red mud (SRM) was tested as a catalyst for the hydrogenation of anthracene oil (a fraction obtained by distillation of coal tar, containing two- to four-ring condensed aromatic

*Corresponding author. Tel.: +34-98510-3508; fax: +34-98510-3434; e-mail: fds@sauron.quimica.uniovi.es

0926-860X/99/$ – see front matter
PII: S0926-860X(98)00373-1

hydrocarbons) [6], and its deactivation for this reaction was studied [7]. The studies of the evolution with time of the red mud activity were carried out at constant temperature (623 K), pressure (10 MPa) and flow rates (hydrogen 4×10^{-6} Nm^3/s, liquid feed 0.6 ml/min at room conditions). Catalyst samples were collected after different reaction times and characterised by BET nitrogen adsorption, scanning electron microscopy (SEM), and SEM-EDX. It was found that sulphided red mud lost its catalytic activity after 40 h reaction time. The loss of catalytic activity of the sulphided red mud was explained by a combination of the loss of BET surface area (45% lost in the 40 h period), and the loss of superficial iron content, measured by EDX maps (74% loss in the 40 h period).

Several methods have been proposed for enhancing red mud catalytic activity. Pratt and Christoverson [1] proposed a dissolution–precipitation method, which decreases the Ca and Na red mud content, and increases its surface area. Red mud modified by the method of Pratt and Christoverson will be referred to in this work as ''activated red mud'', ARM. Sulphided activated red mud (SARM) was tested as a catalyst for the hydrogenation of anthracene oil [12,15], and was found to be both more active than untreated sulphided red mud for the hydrogenation of acenaphthene, anthracene, phenanthrene, fluoranthene and pyrene, as well as presenting an extended active life (approx. 53 h).

In the present work, a new activation method of red mud, based on the method proposed by Pratt and Christoverson, is presented. The new proposed method allows the addition of phosphorous to the catalyst. Phosphorous has been shown to be a very effective promoter for the non carbon-supported sulphide catalysts. Phosphorous has two different promotional effects: it increases the stability of inorganic supports [17], and it improves the dispersion of the active phase [20–23]. However, phosphorus can also be a strong catalyst poison, since it can react with hydrogen yielding phosphine, that chemisorbs strongly on the active sites. This effect is important in carbon-supported catalysts, but is not important in alumina supported catalysts [22,28], since the strong phosphorous–metal oxide interaction avoids the reduction of phosphorous. Another promotional effect of phosphorous reported in the literature is its ability to minimise the poisoning caused by metals present in coal and oil fractions (i.e. vanadium) [25]. Although the promotional effect of phosphorous on the activity of sulphided catalysts has been extensively studied [21,28], to our knowledge the effect of phosphorous on catalyst life has not been documented.

Red mud samples activated by the new method were characterised by BET nitrogen adsorption, X-ray diffraction, scanning electron microscopy (SEM), and SEM-EDX, and after sulphidation, tested as catalysts (activity and life) for the hydrogenation of a light fraction of an anthracene oil. Their catalytic performance is compared with that of sulphided untreated red mud and sulphided red mud activated by the method of Pratt and Christoverson.

2. Experimental

2.1. Materials

The red mud used in this work was supplied by the San Ciprián (Lugo, Spain) plant of the Spanish aluminium company Inespal. Its composition, determined by atomic absorption spectrometry and volumetric methods after acid dissolution and alkaline fusion (details of the analytical method can be found in [12,13]), is given in Table 1.

Reaction studies were carried out by hydrogenating a light fraction of anthracene oil supplied by Nalon-Chem (Asturias, Spain), the composition of which is given in Table 2. The most important compounds are phenanthrene, fluoranthene, pyrene, acenaphthene, fluorene and anthracene. Gaseous reactants were hydrogen N-50, and a mixture of 10.7% hydrogen sulphide and 89.3% hydrogen (vol%) for sulphiding the catalysts.

2.2. Red mud activation

The method of Pratt and Christoverson for enhancing the catalytic activity of red mud consists of dissolving the red mud in aqueous hydrochloric acid, boiling the resulting solution for 2 h, and producing a precipitate by adding aqueous ammonia until pH=8. The precipitate is then filtered, washed with distilled water, dried at 383 K, and calcined in air at 773 K for 2 h [1,15]. This method decreases the content of

Table 1
Bulk and EDX composition of red mud samples (wt %)

Element	RM		ARM		PARM-1		PARM-2	
	Bulk	EDX	Bulk	EDX	Bulk	EDX	Bulk	EDX
Fe	19.7	21.7	25.1	28.9	23.6	27.5	23.0	26.8
Ti	13.0	11.9	16.1	12.8	14.5	11.6	14.1	11.5
Al	7.9	7.4	9.0	7.9	8.4	9.3	7.9	8.2
Na	3.7	3.0	0.1	0.4	0.0	0.0	0.0	0.0
Ca	5.1	4.9	0.9	4.1	2.0	3.9	2.1	4.1
Si	4.7	3.6	4.9	2.7	4.1	3.6	3.8	3.3
P	0.1	0.7	0.2	0.7	3.9	3.1	7.6	6.9

Table 2
Composition of anthracene oil (wt%)

Naphthalene	4.0
Acenaphthene	5.9
Dibenzofuran	3.1
Fluorene	4.9
9,10-Dihydroanthracene	0.8
Phenanthrene	18.2
Anthracene	4.4
Carbazole	2.9
Fluoranthene	10.2
Pyrene	6.2
2-Methylnaphthalene	1.0
Dibenzothiophen	1.2
Methylanthracene	1.1
Methylphenanthrene	1.2
Methylpyrene	1.5
Chrysene	1.7
Triphenilene	1.8

calcium and sodium in the catalyst (Table 1), and increases its surface area (sodium is known to enhance sintering [16]) (Table 3). The activation method presented in this work consists of dissolving the red mud in a mixture of aqueous hydrochloric acid and orthophosphoric acid (H_3PO_4). The subsequent treatments are the same as that in the method of Pratt and Christoverson: precipitation with ammonia, filtering, washing, drying and calcining. Red mud activated by this method (phosphorous-activated red mud, PARM) contains different amounts of phosphorous, depending on the proportion of phosphoric acid in the dissolving solution.

2.3. Catalyst characterisation

The catalyst pore structure and surface area was measured by nitrogen adsorption with a Micromeritics Asap 2000 apparatus.

Catalyst morphology was studied by SEM in a JSM-6100 apparatus. The SEM apparatus is equipped with a Link X-ray microanalyser that provides a quantitative chemical analysis of a catalyst surface layer to a depth of about 1 micron, and supplies information on the superficial distribution of certain elements, providing maps in which the brightness of every pixel depends on the concentration of this element. Catalyst samples must be gold-coated for morphological examination, and polished and carbon-coated for EDX studies.

X-ray diffraction studies were carried out using Siemens D 5000 and Philips PW1729/1710 dust diffractometers, both provided with monochromator and sparkling detectors.

Table 3
Textural characteristics of different red mud samples, obtained by nitrogen adsorption

	RM	SRM	ARM	SARM	PARM-1	SPARM-1	PARM-2	SPARM-2
BET surface (m^2/g)	24.3	29.5	82.4	85.4	80.4	82.0	77.1	79.6
BJH desorption pore volume (cm^3/g)	0.086	0.090	0.227	0.170	0.198	0.188	0.181	0.174
BET average pore diameter (nm)	12.1	10.5	9.8	8.6	8.8	10.6	8.4	9.7

2.4. Reaction studies

The reactor used for the hydrogenation experiments was a cylindrical stainless steel continuous packed bed reactor with 9 mm internal diameter and 45 cm long. Two grams of catalyst was placed in the central section of the reactor, the upper and lower sections being filled with low-area inert alumina. The catalysts were sulphided in situ before use by passing a mixture of 10% hydrogen sulphide in hydrogen at atmospheric pressure, heated to 673 K, through the reactor for 4 h. The reactor was operated as a continuous trickle bed reactor, liquid and gas feeds flowing concurrently downwards. The liquid feed consisted of 20 wt% anthracene oil dissolved in toluene for easier handling, containing 1 wt% carbon sulphide, added to maintain the catalyst in the sulphided form. The gas feed consisted of high pressure hydrogen. Reaction products were collected in a cylindrical receiver, and liquid samples were withdrawn by emptying the receiver at different time intervals. Hydrogenated anthracene oil was analysed by gas chromatography using a capillary fused silica column with apolar stationary phase SE-30, and the peak assignment was performed by gas chromatography–mass spectrometry. Reactions were carried out under the same conditions as the experiments using SRM [7], and SARM [15]: pressure 10 Mpa, temperature 623 K, hydrogen flow rate 4×10^{-6} N m^3/s, and liquid flow rate (at room conditions) 0.6 ml/min. Further details of the experimental set up and procedure of the reaction are given in [6].

3. Results and discussion

3.1. Catalysts characterisation

Several samples of PARM were produced, with different phosphorous content. The composition of two samples containing approx. 4% and 8% phosphorous (which will be referred to here as PARM-1 and PARM-2, respectively), are given in Table 1. Both ARM and PARM samples show a similar decrease in sodium content, while the calcium content is higher in PARM samples than in ARM.

The results of textural characterisation by nitrogen adsorption for the catalyst samples, unsulphided and sulphided, are given in Table 3 and Fig. 1. The surface area was calculated according to the Brunauer, Emmet and Teller method, while the pore volume was calculated using the method of Barret, Joyner and Halenda [16]. The average pore diameter was calculated as 4×(pore volume)/(surface). The surface area and pore volume of the phosphorous-containing samples, although much higher than that of RM, are slightly lower than that of ARM, the surface area decreasing as the phosphorous content increases. Samples prepared with higher phosphorous content than PARM-1 and PARM-2 decreased the surface area (61.3 m^2/g for the sample with 15% phosphorous). This behaviour, which is in agreement with results reported for other sulphided catalysts [17], suggest a crystallographic reordering, or pore blockage, precipitation of phosphate ions [20].

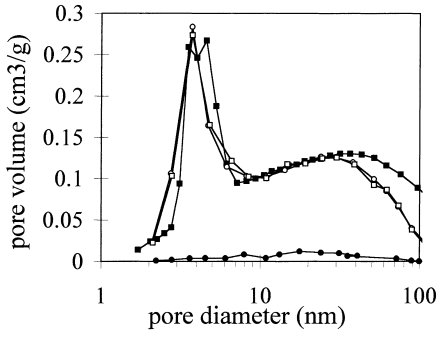

Fig. 1. Pore volume distributions of: RM (●); ARM (■); PARM-1 (○); PARM-2 (□).

The following red mud constituents were identified by X-ray diffraction: rutile, TiO_2; hematite, Fe_2O_3; goethite and lepidocrocite, FeO(OH); iron hydroxide, $Fe(OH)_3$; halloysite, $Al_2Si_2O_5(OH)_4$; and bayerite, $Al(OH)_3$. The effect of the activation methods and sulphidation on these constituents is shown in Fig. 2. PARM-1 and ARM diffractograms are very similar. Both activation methods eliminate all the aluminium containing crystalline forms (bayerite and halloysite), and the iron containing forms lepidocrocite and iron hydroxide. Goethite decreases in ARM, while it disappears completely in PARM-1. PARM-1 also shows a new unidentified peak, which probably is associated with a complex phase of iron, phosphorous and aluminium. Ramselaar et al. [27] found similar phases in phosphorous-promoted Fe_2O_3/γ-Al_3O_3 catalysts using Mossbauer spectroscopy.

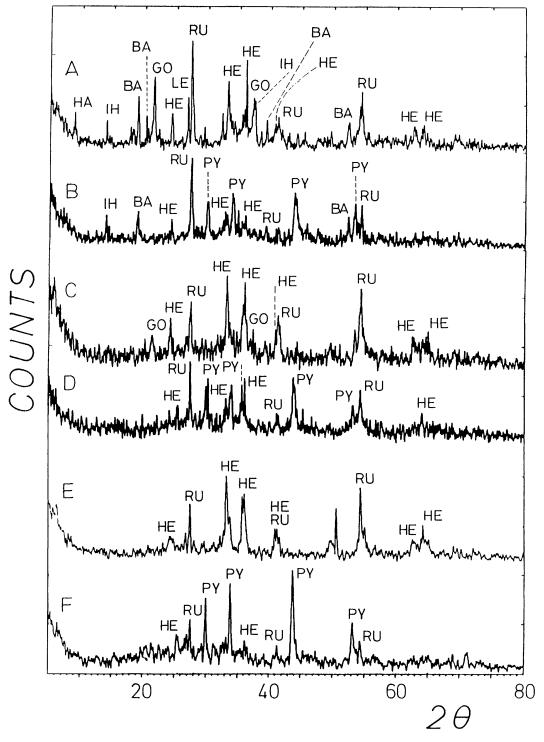

Fig. 2. X-ray diffractograms for: (a) RM; (b) SRM; (c) ARM; (d) SARM; (e) PARM-1; (f) SPARM-1.

Sulphidation forms pyrrhotite ($Fe_{(1-x)}S$), and decreases the crystalline iron oxides and hydroxides content. This effect is more pronounced for SPARM-1, which exhibits a higher pyrrhotite content and a lower hematite content than SARM. Pyrrhotite is a non-stoichiometric sulphide, nominally Fe_7S_8, with a regular NiAs structure. This structure has "iron vacancies" (formed by its non-stoichiometric character), that exhibit spatial order. Pyrrhotite is thermodynamically stable at temperatures above 200°C, and is catalytically active in hydrogenation reactions [24].

The high content in pyrrhotite in PARM is tentatively explained considering that the addition of phosphoric acid increases the solubility of Fe (III) into the aqueous solution during the RM activation. When ammonia is added, smaller particles of iron (III) hydroxide precipitate. These particles are more easily sulphided. Mc Cormick et al. [29] stated that diffusional effects play an important role in the sulphidation of iron (II) oxides.

3.2. Reaction studies

Under the reaction condition specified in Section 2, the anthracene oil constituents that were hydrogenated to a measurable degree when using SPARM-1 and SPARM-2 as catalysts, were the same as when using SRM and SARM. These compounds and their respective main reaction products are: anthracene, yielding 9,10-dihydroanthracene and small amounts of 1,2,3,4-tetrahydroanthracene; phenanthrene, yielding 9,10-dihydrophenanthrene; fluoranthene, yielding 1,2,3,10b-tetrahydrofluoranthene; and pyrene, yielding 4,5-dihydropyrene. The hydrogenation of these compounds accounts for more than 75% of the total hydrogen consumption, and no hydrogenation or cracking products of the solvent (toluene) were detected. The evolution of the conversions of the aforementioned compounds with reaction time is shown in Fig. 3 (SPARM-1) and Fig. 4 (SPARM-2).

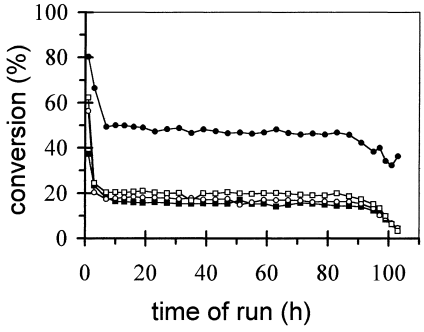

Fig. 3. Conversions versus run time for SPARM-1: anthracene (●); phenanthrene (■); fluoranthene (○); pyrene (□).

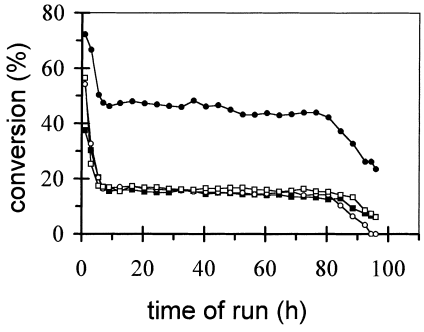

Fig. 4. Conversions versus run time for SPARM-2: anthracene (●); phenanthrene (■); fluoranthene (○); pyrene (□).

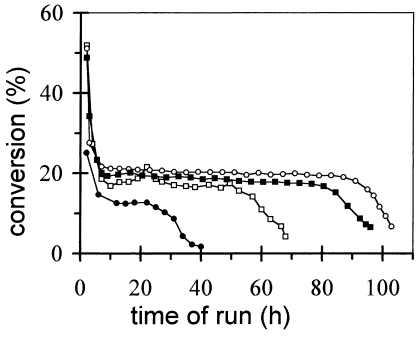

Fig. 5. Average conversions versus run time for: SRM (●); SARM (□); SPARM-1 (○); SPARM-2 (■).

The compound which is hydrogenated to a greater extent is anthracene, while conversions for phenanthrene, fluoranthene and pyrene are very similar. This behaviour is similar to that observed for SARM [15]. The activity and resistance to deactivation of SPARM catalysts can be better compared in Fig. 5, in which average conversions along with those for SRM and SARM are plotted versus reaction time. Average conversion is defined as

$$\text{average conversion} = \frac{\Sigma \text{ compounds in feed} - \Sigma \text{ compounds in product}}{\Sigma \text{ compounds in feed}},$$

where Σ compounds is the sum of the concentrations of anthracene, phenanthrene, fluoranthene and pyrene.

It can be observed that both SPARM catalysts present a slightly higher hydrogenation activity than SARM, and a marked increase in their active life. In fact, while SARM gives a constant conversion for a period of 47 h after the initial period of fast activity decay, the period of constant activity is extended to 75 h for SPARM-2 and to 85 h for SPARM-1. The catalyst containing 4% P (SPARM-1) performs better than the catalyst containing 8% P (SPARM-2), as SPARM-1 is more active and stable. This can be explained considering the decrease in the surface area of SPARM-2 with respect to SPARM-1.

The slightly higher activity of SPARM-1 compared to SARM can be ascribed to the promotional effect of phosphorous in sulphide catalysts supported by inorganic materials. Some authors [23], state that this effect is more important in hydrogenation reactions than in hydrodisplacement reactions. On the other hand, the decrease of activity of SPARM-2 compared to SPARM-1 can be explained by the decrease of surface area.

3.3. Catalyst deactivation

The deactivation of SPARM-1 was studied in different experiments by collecting catalyst samples after 1, 3, 12, 68 and 103 h reaction time, the last sample corresponds to almost completely deactivated catalyst.

The textural evolution with reaction time for SPARM-1 is given in Table 4 and Fig. 6. The surface area decreases sharply during the first 3 h of reaction time, after which it decreases very slowly. The surface area of SPARM during the constant activity period (about 65 m^2/g) is higher than that of SARM (about 50 m^2/g, [12]). These results show the stabilising effect of phosphorous in the catalyst structure.

Fig. 7 shows X-ray diffractograms for SPARM-1 samples collected at different reaction times. The progressive decrease of the pyrrhotite peaks and increase of the hematite peaks are clearly evident. No peaks of intermediate iron compounds as troilite (FeS), pyrite (FeS_2) or magnetite (Fe_3O_4) were found. Since hematite has no catalytic activity for these reactions [18], the decrease in pyrrhotite content can cause the catalyst deactivation. The decrease in

Table 4
Morphological parameters of SPARM-1 after different reaction times

Reaction time						
Parameter	0	1	3	12	68	103
Surface area BET (m^2/g)	82	69.2	66.9	64.4	61.6	54.7
Pore volume BJH-desorption (cm^3/g)	0.188	0.172	0.140	0.161	0.137	0.114
Average pore diameter BET (nm)	10.6	11.3	9.6	10	8.9	8.3

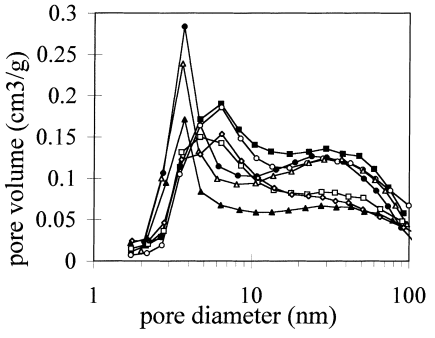

Fig. 6. Pore volume distributions of PARM-1: fresh, unsulphided (●), after 1 h reaction time (○), after 12 h reaction time (△), after 103 h reaction time (▲); fresh, sulphided (■) after 3 h reaction time (□), after 68 h reaction time (◇).

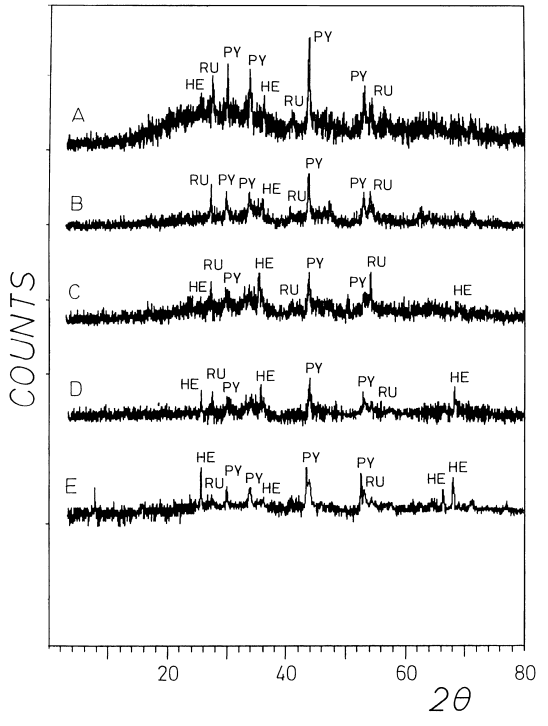

Fig. 7. X-ray diffractograms for SPARM-1 samples after different reaction times: (a) 0 h; (b) 3 h; (c) 12 h; (d) 45 h; (e) 68 h; (f) 96 h.

pyrrhotite occurred even though 1% of carbon disulphide was added to the feed to maintain iron in the sulphided form. Carbon disulphide concentration in the feed was not increased, since the hydrogen sulphide formed inhibits hydrogenation, as it chemisorbs in the same active sites than aromatics [18,19].

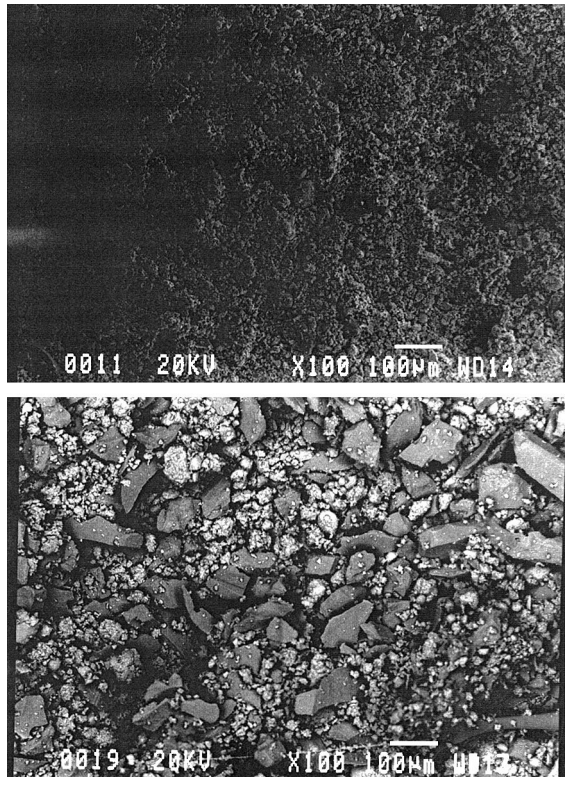

Fig. 8. SEM photographs of the surface of SPARM-1 after: (a) 1 h run time; (b) 103 h run time.

SEM and SEM-EDX studies for SRM [7] and SARM [15] showed that the morphology of the catalysts changed as the reaction proceeded, the iron-containing rather granular uniform surface of fresh catalysts being progressively occupied by flat-surfaced bigger particles, mainly made up of alumina, and the association of titanium, sulphur, silicon and calcium with iron. The same trends, although the transformation was slower, can be observed for SPARM-1 in the SEM photographs of Fig. 8, the SEM-EDX maps of Figs. 9 and 10, and in the concentrations measured by SEM-EDX given in Table 5. The data in Table 5 also show a progressive decrease in the superficial concentration of phosphorous as the reaction proceeds. In EDX maps, the brightness of every pixel is related to the intensity of emission of the characteristic K_α line of each element, and thus to its concentration in the surface layer: white corresponds to a high concentration of a given element, black to the absence of this element, and greys to intermediate

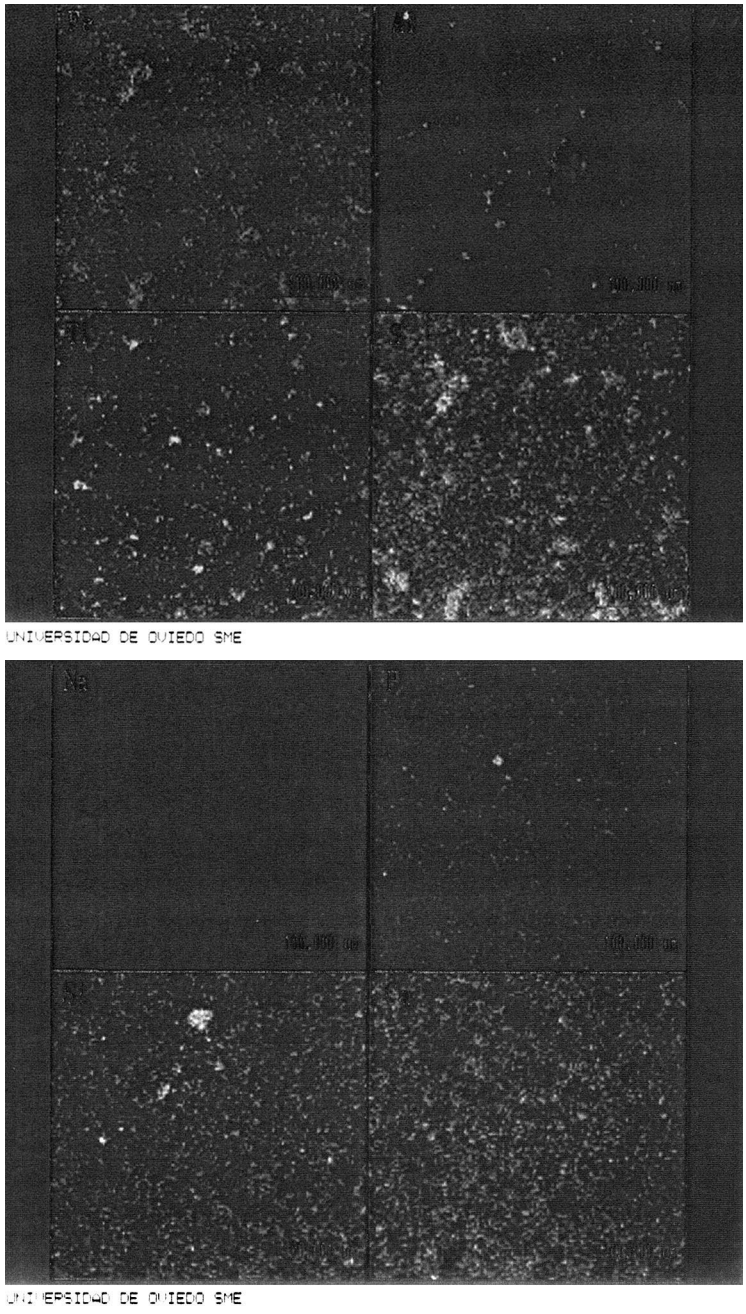

Fig. 9. SEM-EDX maps of distribution of elements of fresh SPARM-1.

concentrations. The pictures corresponding to the elements at high concentrations (iron, aluminium, titanium and sulphur) were obtained by setting a different level of brightness to the ones corresponding to the elements at low concentrations (sodium, chlorine, silicon and calcium).

The surface iron content decreases with time, as measured by EDX elemental analysis (Table 5). This

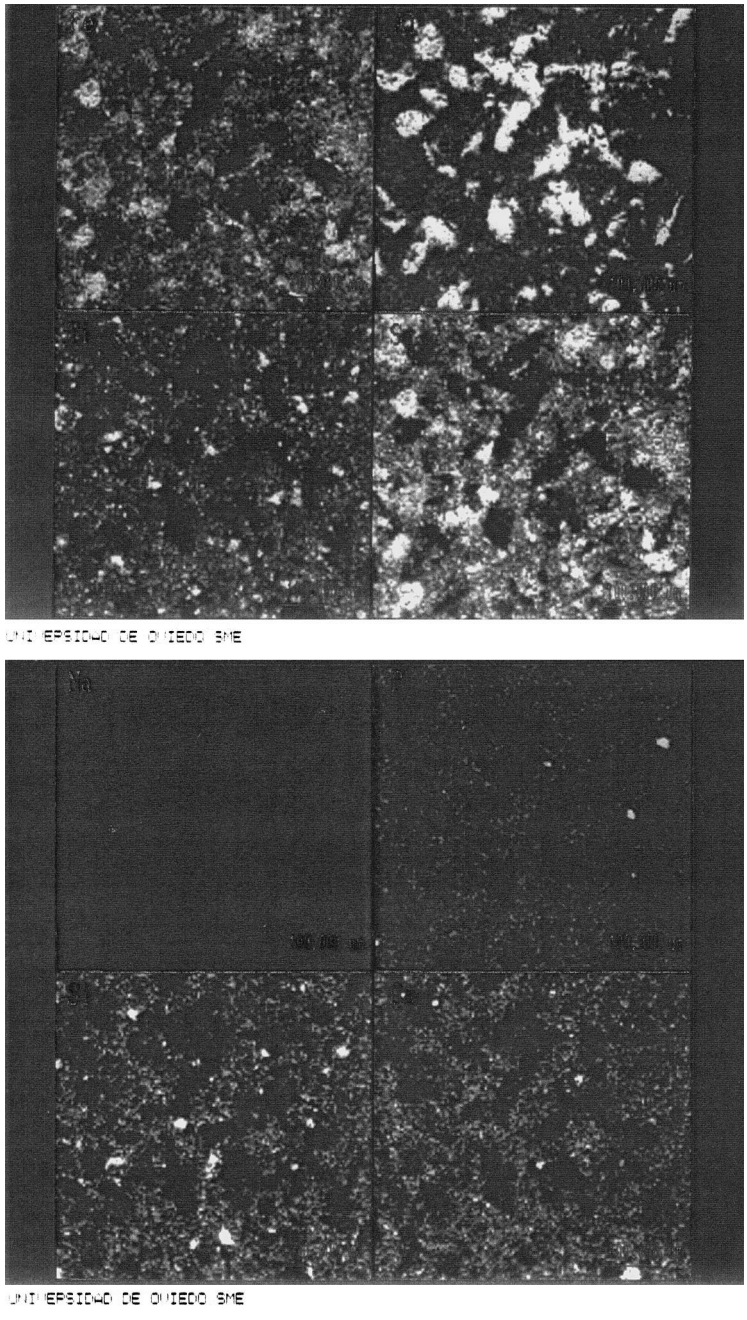

Fig. 10. SEM-EDX maps of distribution of elements of SPARM-1 after 103 h reaction time.

effect, which is also observed in the experiments with RM and ARM, [7,15], may be due to diffusion of aluminium to the surface and/or iron to the bulk phase. Ramselaar et al. [27] deduced, using Mossbauer spectroscopy and working with iron sulphides supported on alumina, that some of the iron could diffuse into the alumina support under typical hydrotreatment conditions (T>573 K), yielding an inactive Fe(II)-alumi-

Table 5
EDX composition of SPARM-1 after different reaction times (wt%)

Reaction time						
Element	0 h	1 h	3 h	12 h	68 h	103 h
Fe	37.8	38.4	35.7	33.8	30.1	29.1
Ti	17.0	16.1	14.8	13.1	13.2	13.8
S	20.1	21.1	20.1	21.1	19.8	20.6
Al	12.1	11.7	13.5	15	20.1	23.4
Ca	5.0	4.8	4.9	5.7	5.8	4.2
Si	5.8	4.4	7.0	7.8	7.3	6.4
Na	0.6	0.6	0.6	0.6	0.6	0.4
Cl	0.0	0.0	0.0	0.1	0.2	0.3
P	3.0	2.9	2.9	2.4	2.1	1.6
V	0.2	0.2	0.2	0.2	0.3	0.2

nate. Decrease of iron content by volatilisation is unlikely, since neither in the feed nor in the catalyst there are anions capable to favour volatilisation of iron. Furthermore, studies of red mud as hydrodechlorination catalyst in the presence of important amounts of hydrogen chloride, showed that this phenomenon is not important, chlorides being the most volatile iron salts [26].

Deactivated SPARM, (after 103 h reaction time), was washed in a Soxhlet apparatus with toluene and cyclohexene, and reused without previous re-sulphidation. Results (Fig. 11), show some recovery of catalytic activity. Since catalyst washing mainly cleans carbonaceous deposits, it is possible that fouling of the catalytic surface also plays a role in catalyst deactivation.

According to these results, the deactivation of SPARM-1 may be caused by the combination of the decrease in surface area (due to sintering and/or coke deposition), decrease in superficial iron content, and the transformation of pyrrhotite into hematite.

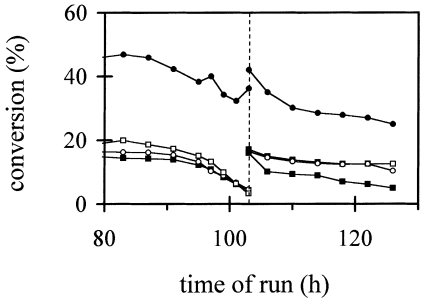

Fig. 11. Conversion of washed PARM (before washing at the left of dashed line, and after washing at the right of dashed line): anthracene (●), phenanthrene (■), fluoranthene (○), pyrene (□).

4. Conclusion

The activation method presented in this work has proved to be more effective in improving the performance of red mud as a hydrogenation catalyst than the method of Pratt and Christoverson, as the activated catalyst presents a slightly higher level of activity and a markedly extended active life.

Acknowledgements

This work has been supported by the Spanish Interministerial Commission for Science and Technology under grant MAT92-0807. The authors are grateful to Mr. Alfredo Quintana of the Electron Microscopy Service of the University of Oviedo, and to Dr. Amelia Martínez and Dr. Juan M. Díez Tascón of the Instituto Nacional del Carbón Manuel Pintado Fe (CSIC, Oviedo).

References

[1] K.C. Pratt, V. Christoverson, Fuel 61 (1982) 460.
[2] A. Eamsiri, R. Jackson, K.C. Pratt, V. Christov, M. Marshall, Fuel 71 (1992) 449.
[3] D. Garg, E.N. Givens, Ind. Eng. Chem. Proc. Des. Dev. 24 (1985) 66.

[4] S. Sato, M. Morita, T. Hashimoto, I. Mitunori, K. Chiba, H. Tagaya, Fuel 68 (1989) 622.
[5] B. Klopties, W. Hodek, F. Bandermann, Fuel 69 (1990) 448.
[6] J.J. Llano, R. Rosal, H. Sastre, F.V. Díez, Fuel 73 (1994) 688.
[7] J. Alvarez, R. Rosal, H. Sastre, F.V. Díez, Appl. Catal. A 128 (1995) 259.
[8] D.D. Whitehurst, D.O. Mitchell, M. Farcasiu, Coal Liquefaction, Academic Press, New York, 1980.
[9] K. Chiba, H. Tagoya, T. Kobayashi, Y. Shibuya, Ind. Eng. Chem. Res. 26 (1987) 1329.
[10] S.E. Moschopedis, J.G. Hawkins, J.F. Fryernad, J.G. Speight, Fuel 59 (1980) 647.
[11] T. Yotono, H.D. Marsh, in: H.D. Schultz (Ed.), Coal Liquefaction Products: NMR Spectroscopic Characterization and Production Processes, Wiley, New York, 1983, p. 125.
[12] J. Alvarez, Ph.D. Dissertation, University of Oviedo, Oviedo, 1995.
[13] R. Rosal, F.V. Díez, H. Sastre, Fuel 71 (1992) 761.
[14] R. Rosal, F.V. Díez, H. Sastre, Ind. Eng. Chem. Res. 31 (1992) 1007.
[15] J. Alvarez, R. Rosal, F.V. Díez, H. Sastre, Appl. Catal. A 167 (1998) 215.
[16] C.N. Satterfield, Heteregeneous Catalysis in Industrial Practice, McGraw-Hill, New York, 1981.
[17] K. Gischti, S. Ianibello, G. Marengo, G. Morelli, P. Tittarelli, Appl. Catal. A 12 (1984) 391.
[18] J.J. Llano, Ph.D. Dissertation, University of Oviedo, Oviedo, 1993.
[19] M.J. Girgis, Ph.D. Dissertation, Universty of Delaware, 1988.
[20] R. López-Cordero, N. Esquivel, J. Lázaro, J.L.G. Fierro, A. López-Agudo, Appl. Catal. 48 (1989) 341.
[21] J.L.G. Fierro, A. López-Agudo, N. Esquivel, R. López-Cordero, App. Catal. 48 (1989) 353.
[22] S.M.A.M. Bouwens, J.P.R. Vissers, V.H.J. de Beer, R. Prins, J. Catal. 112 (1988) 401.
[23] H. Tapsøe, B.S. Clausen, F.E. Massoth, in: J.R. Anderson, M. Boudart (Eds.), Catalysis: Science and Technology XI, Springer, Heidelberg, 1996, p. 193.
[24] W.L.T.M. Ramselaar, V.H.J. de Beer, A.M. Van de Kraan, Appl. Catal. 42 (1988) 153.
[25] S. Kushiyama, R. Aizawa, S. Kobayashi, Y. Koinuma, I. Uemasu, H. Ohuichi, Appl. Catal. 63 (1990) 279.
[26] S. Ordóñez, F.V. Díez, H. Sastre, Communication to SECAT'97 (Spanish Society of Catalysis), Jaca, 1997.
[27] W.L.T.M. Ramselaar, M.W.J. Craje, R.H. Hadders, E. Gerkema, V.H.J. de Beer, A.M. Van de Kraan, Appl. Catal. 65 (1990) 69.
[28] W.L.T.M. Ramselaar, S.M.A.M. Bouwens, V.H.J. de Beer, A.M. Van de Kraan, Hyp. Interact. 46 (1989) 599.
[29] S. McCormick, M.A. Dayananda, R.E. Grace, Met. Trans. B 6b (1975) 55.